Enhancement of low power CO2 laser cutting process for injection molded polycarbonate

Moradi, M., Mehrabi, O., Azdast, T. & Benyounis, K. Y.

Original citation & hyperlink:
Moradi, M, Mehrabi, O, Azdast, T & Benyounis, KY 2017, 'Enhancement of low power CO2 laser cutting process for injection molded polycarbonate', Optics and Laser Technology, vol. 96, pp. 208-218.
https://dx.doi.org/10.1016/j.optlastec.2017.05.022

DOI 10.1016/j.optlastec.2017.05.022
ISSN 0030-3992

Publisher: Elsevier

Enhancement of low power CO_2 laser cutting process for injection molded polycarbonate

Mahmoud Moradi[1, 2]*, Omid Mehrabi[1, 2], Taher Azdast[3], Khaled Y. Benyounis[4]

1- Department of Mechanical Engineering, Faculty of Engineering, Malayer University, Malayer, Iran, Omidmehrabi70@gmail.com

2- Laser Materials Processing Research Center, Malayer University, Malayer, Iran

3- Department of Mechanical Engineering, Urmia University, Urmia, Iran, taherazdast@gmail.com

4- School of Mech. & Maun. Eng., Dublin City University, Dublin, Ireland, khaled.benyounis2@mail.dcu.ie

Abstract

Laser cutting technology is a non-contact process that typically is used for industrial manufacturing applications. Laser cut quality is strongly influenced by the cutting processing parameters. In this research, CO_2 laser cutting specifications have been investigated by using design of experiments (DOE) with considering laser cutting speed, laser power and focal plane position as process input parameters and kerf geometry dimensions (i.e. top and bottom kerf width, ratio of the upper kerf to lower kerf, upper heat affected zone (HAZ)) and surface roughness of the kerf wall as process output responses. A 60 Watts CO2 laser cutting machine is used for cutting the injection molded samples of polycarbonate sheet with the thickness of 3.2 mm. Results reveal that by decreasing the laser focal plane position and laser power, the bottom kerf width will be decreased. Also the bottom kerf width decreases by increasing the cutting speed. As a general result, locating the laser spot point in the depth of the workpiece the laser cutting quality increases. Minimum value of the responses (top kerf, heat affected zone, ratio of the upper kerf to lower kerf, and surface roughness) are considered as optimization criteria. Validating the theoretical results using the experimental tests is carried out in order to analyze the results obtained via software.

Keywords: Laser Cutting; Statistical investigation; modelling and optimization; injection molding; Design of experiments

[1] * moradi@malayeru.ac.ir
P. O. Box 65719-95863 Malayer, Iran

1. Introduction

In laser cutting the focused laser beam is directed onto the surface of the work piece to rapidly heat it up, resulting in melting and/or vaporization, depending on the beam intensity and work piece material .The molten and/or vapor is then blown away using an assist gas [1, 2, 3].

Thermoplastics are increasingly being used in biomedical, automotive and electronics industries due to their excellent physical and chemical properties [4]. In particular, thermoplastics offer significant advantages over thermoset and elastomer because of their fatigue resistance and high fracture toughness upon reheating and remolding processes. As the name implies, thermoset cannot be reheated and remolded once formed. Although elastomer possesses exceptional elastic property, it is limited to applications where large deformation is soughed while structural rigidity is compromised and thus it is being used in flexible tubing. An example of mostly used engineering thermoplastics is polycarbonate (PC) [1, 4].

Performing experiments based on trial and error takes much time and does not consider the interactions of parameters, causing lots of errors. Recently, design of experiments (DOE) has been developed in various experimental works [5, 6]. Reduction in the number of experiments, consideration of interaction effects and development of mathematical functions to achieve the logical relationship between input and output parameters are the advantages of applying response surface methodology (RSM) [7,8]. Also neural networks are one of the most proper tools in artificial intelligence which are widely used in industry applications [9, 10]. The complex relationships between control variables and response variables could not be determined by any analytic model. Bharti et al [11] declared that neural networks have been shown to be an effective technique for modeling complex nonlinear processes. They are useful for functional prediction and system modeling where the processes are not understood or are highly complex. The neural network can be trained to perform a particular function by adjusting the values of the connections (weights) between elements.

Zhou and Mahdavian [12] studied on the capability of low power laser to perform tasks other than marking. A theoretical model was developed to estimate the depth of cut with the cutting velocity and laser power for several materials. The agreement between theoretical and experimental results was investigated for a different range of materials. This research has demonstrated that low power (60 W) CO_2 laser can be used for cutting nonmetallic materials and they are particularly suitable for plastic board cutting. Patel et. al. [13] investigated experimental

analysis and prediction of kerf width in laser cutting of glass fiber reinforced plastic composite material and developed regression and artificial neural network (ANN) models to predict the kerf width for specific range of inputs. Pathik Patel et al [14] presented experimental analysis and ANN modelling of heat affected zone in laser cutting of glass fiber reinforced plastic composites. Tomomasa Ohkubo et al [15] studied the numerical simulation of laser beam cutting of carbon fiber reinforced plastic (CFRP). The effect of process parameters and optimization of CO_2 laser cutting of ultra-high-performance polyethylene was reported by Eltawahni et al [16]. The aim of this work was to relate the cutting edge quality parameters (responses) namely: upper kerf, lower kerf, ratio of the upper kerf to lower kerf and cut edge roughness to the process parameters considered in this research and to find out the optimal cutting conditions. The process factors implemented in this research are laser power, cutting speed and focal point position. Laser machining of composites in terms of scope, limitation and application and the research carried out for different types of polymer composites [17]. Ayob Karimzad et al [18] studied the effect of carbon nanotubes on injection molded multi-walled carbon nanotubes/poly methyl methacrylate (MWCNT/PMMA) composite in CO_2 laser cutting quality. Also the effect of processing parameters on laser cutting of MWCNT/PMMA nanocomposites was investigated using full factorial design. Weight percent of MWCNT in four levels, laser power in three levels and federation three levels, were considered as the input variables while heat affected zone (HAZ), the average kerf width, and the taper kerf of the sample were measured as output responses .Choudhury and Chuan [19] surveyed laser cut quality of glass fiber reinforced plastic composite experimentally. Eltawahni et al [20-22] investigating the CO_2 laser cutting parameters of MDF, plywood and PMMA material based on the design of experiments (DOE) approach. In another research Eltawahni et. al [23] studied CO_2 laser cutting of medical grade AISI316L. Mathematical models were developed to determine the relationship between the process parameters and the edge quality features. Process optimization was conducted to find out the optimal cutting setting that would enhance the quality or minimize the operating cost. Laser cutting of carbon fiber reinforced plastics (CFRP) of high thickness was investigated based on a remote cutting approach to generate high process speeds and reduce heat affected zones to around 200 μm. [24]. The estimation of the most influential factors of the laser cutting process on the heat affected zone (HAZ) by adaptive neuro-fuzzy technique was reported by dalibor petkovic et. al [25].

In the present study, RSM as one of the best DOE methods used to analyze the effect of the three input CO_2 laser cutting process variables, i.e. laser focal plane position (FPP), the cutting speed (S) and the laser power (P) on the geometry and surface roughness of the kerf wall in the samples of polycarbonate injection molded sheets with thickness of 3.2mm. Figure 1 displays a schematic view of the kerf geometrical characteristics created by laser on the polycarbonate sheets. Top and bottom kerf width, ratio of the upper kerf to lower kerf, upper heat affected zone (HAZ) as well as surface roughness of the kerf wall were measured and analyzed by statistical software, MINITAB 17. Optimization of the laser cutting parameters was carried out to obtain proper geometrical feature and surface roughness of the cut kerf. In order to validate the optimization results, five cutting experiments were conducted at optimum settings and compared with the software optimization results.

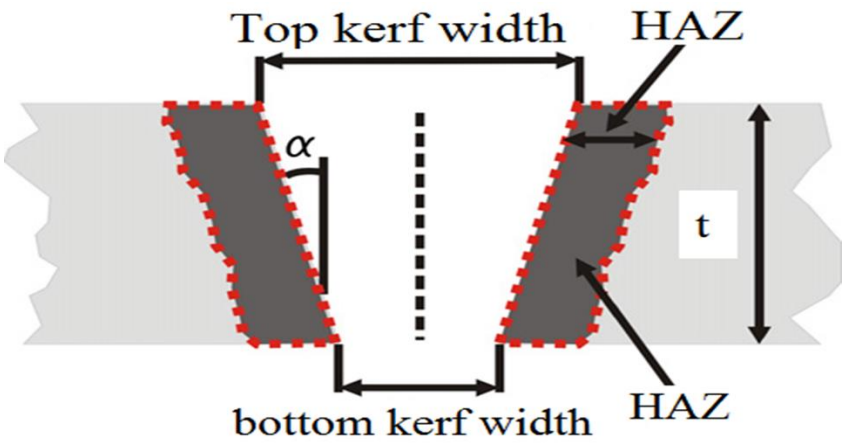

Figure. 1. Geometrical features of the cross-section of the kerf [26]

2. Experimental Design and Methodology

2.1 Response surface methodology (RSM)

Response Surface Methodology (RSM) is a set of statistical techniques and applied mathematics to investigate responses (output variables) which are affected by a number of independent variables (input variables) [27]. In each experiment, changes in input variables are made in order to determine the cause of changes in the response variable. And the purpose is to find a relationship between outputs and inputs (responses and parameters) with a minimum of errors in the form of a mathematical model. Depending on the type of input variable parameters there are

in general different ways to design an experiment. In the present study, Response Surface Methodology is chosen as the method of design. When all the independent variables are capable of being measured and controlled during an experiment, the response surface is to be expressed as a function through Equation 1 [28, 29].

$$Y = f(x_1, x_2, x_3, \ldots, x_k) \quad (1)$$

Here, "k" is the number of independent variables. Finding a rational function to relate the independent variables to the responses seems essential. Therefore, usually a quadratic polynomial function presented in Equation 2 is applied in response surface methodology [30, 31].

$$y = \beta_0 + \sum_{i=1}^{k} \beta_i x_i + \sum_{i=1}^{k} \beta_{ii} x_i^2 + \sum_{i} \sum_{j} \beta_{ij} x_i x_j + \varepsilon \quad (2)$$

In the above equation, β is constant, βi is linear coefficients, βii is coefficients of quadratic, βij is interaction coefficients and ε is the error of the parameters of regression. In this research, laser focal plane position (FPP), the cutting speed (S) and the laser power (P) were considered as independent input parameters. Table 1 shows three input variables of the experiment, coded values and actual values of their levels. The focal plane position (FPP) was considered as zero when it was set on upper the material surface. Above or below the upper surface the FPP was considered as positive or negative respectively. Schematic diagram of the FPP is illustrated in figure 2. In the present study, in order to perform the experiments, central composite design (CCD) five-level RSM design with three parameters, presented in Table 2, were applied. The experimental design includes 17 experiments which include eight experiments as factorial points in the cubic vertex, six experiments as axial points and three experiments in the cubic centre as centre point experiments.

Table 1. Independent process parameters with design levels

Variable	Notation	Unit	-2	-1	0	1	2

Cutting speed	S	[mm/s]	2	6	10	14	18
Laser power	P	[w]	20	25	30	35	40
Focal plane position	FPP	[mm]	0	-1	-2	-3	-4

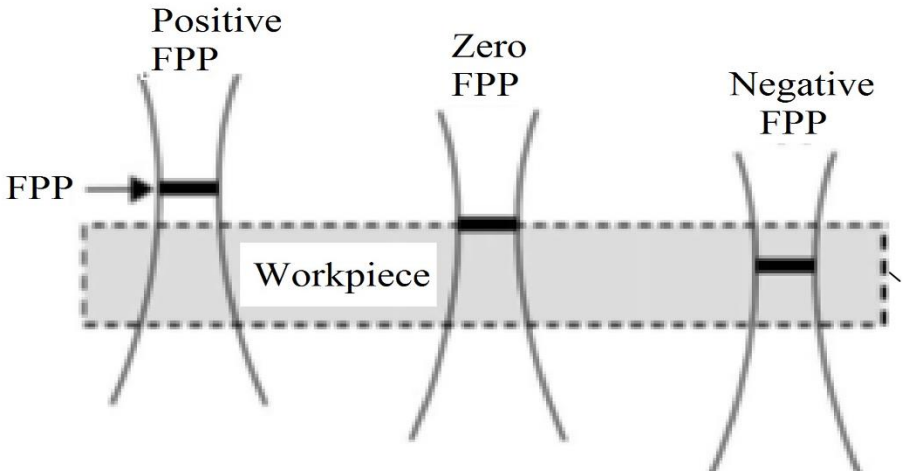

Figure. 2. Variation of focal Plane position on the work piece [32]

Table 2. Experimental layout and multi-performance results

Experiment No.	Input variables (Coded values)			Output responses				
	Cutting speed [-]	Laser power [-]	Focal plane position [-]	Top kerf [µm]	Bottom kerf [µm]	Ratio [---]	Heat effect zone [µm]	Surface roughness [µm]
1	-1	1	-1	265.30	163.26	1.6250	265.30	3.32
2	2	0	0	303.34	154.35	1.9652	235.67	6.9
3	0	0	0	312.24	163.26	1.9151	275.51	5.41
4	0	0	0	306.12	161.22	1.8987	279.59	3.72
5	0	0	-2	318.36	126.53	2.5161	253.06	4.81
6	0	0	2	357.60	185.450	1.9282	285.350	6.81
7	1	-1	1	299.35	157.88	1.8960	178.67	5.36
8	1	-1	-1	❋	❋	❋	❋	❋
9	-1	-1	1	376.64	318.37	1.1538	306.12	5.15
10	-1	-1	-1	265.30	244.90	1.0833	316.12	2.15
11	1	1	-1	295.31	171.43	1.7261	257.14	2.92
12	0	0	0	397.95	183.67	1.7415	248.94	4.89
13	0	2	0	387.75	244.90	1.5833	224.48	3.28
14	1	1	1	305.83	180.340	1.6958	277.89	2.92
15	-2	0	0	306.12	387.75	0.7894	420.49	6.13

16	0	-2	0	❋	❋	❋	❋	❋
17	-1	1	1	518.37	363.26	1.4269	330.61	9.74

2.2 Desirability approach

Many response surface problems involve the analysis of several responses. Simultaneous consideration of multiple responses involves first building an appropriate response surface model for each response and then trying to find a set of operating condition that in some sense optimizes all responses or at least keeps them in desired ranges. The desirability method is recommended due to its simplicity, availability in the software and provides flexibility in weighting and giving importance for individual response. Desirability method is a simultaneous optimization technique which popularized by Drringer and Suich in 1980 [33]. Solving such multiple response optimization problems employing this technique involves using a technique for combining multiple responses into a dimensionless measure of performance called the overall desirability function [34]. The general approach is to first convert each response Yi into a unitless utility bounded by $0<di<1$, where a higher di value indicates that response value Yi is more desirable, and if the response is outside an acceptable region, di=0. Then the design variables are chosen to maximize the overall desirability [33]:

$$D= (d_1.d_2….d_m)^{1/m} \quad (3)$$

Where, m is the number of responses. In the current work, the individual desirability of each response, di, was calculated using Eqs. (4-6). the shape of the desirability function depends on the weight field ‘r’. Weights are used to emphasize the target value. When the weight value is equal to 1, this will make the desirability function in linear mode. Choosing r>1 places more

emphasis on being close to the target value, and choosing 0<r<1 makes this less important [33, 34]. If the target T for the response y is a maximum value, the desirability will be defined by:

$$d = \begin{cases} 0 & y < L \\ \left(\frac{y-L}{T-L}\right)^r & L \le y \le T \\ 1 & y > T \end{cases} \quad (4)$$

For goal of minimum, the desirability will be defined by:

$$d = \begin{cases} 1 & y < L \\ \left(\frac{T-y}{T-L}\right)^r & L \le y \le T \\ 0 & y > T \end{cases} \quad (5)$$

If the target is located between the lower (L) and upper (U) limits, the desirability will be defined by

$$d = \begin{cases} 0 & y < L \\ \left(\frac{y-L}{T-L}\right)^r & y < L \\ \left(\frac{T-y}{T-L}\right)^r & L \le y \le T \\ 0 & y > T \end{cases} \quad (6)$$

3. Experimental Design and Methodology

In order to inject the polycarbonate sheets a mold containing two cavities with dimension of 175×80×3.2 mm are used, Figure 3. Polycarbonate sheets are produced using an NBMHXF-128 plastic injection molding machine. Injection and holding pressures of the process was set at 85 and 110 bar, respectively, and the temperatures of barrel zones are set at 270,290,320 and 320 1C. Laser cutting of the polycarbonate sheets is conducted using a continuous wave CO_2 Rabbit HX-1290SE laser with maximum 60 Watts power.

Figure. 3. Used mold for injecting the polycarbonate specimens

There are various ways in which the focal position is determined. In one acrylic sheet mounted at 80 degree to the horizontal is traversed horizontally to cross the vertical beam. The imprint of the beam on the sheet identifies the location of the focal point [35]. Figure 4 depicts the determining the focal plane position of the used laser machine.

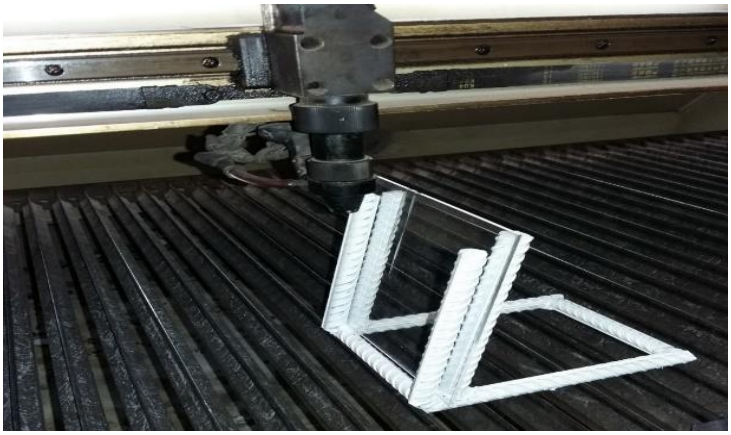

Figure. 4. Experimental determining the focal plane position of the used CO_2 laser machine

Trial specimens of laser cutting were performed by varying one of the process variables to determine the working range of each parameter. Narrow kerf width and complete cutting were the criteria used for choosing the working ranges [36]. Laser cutting experiments were performed according to the matrix scheme of DOE presented in Table 2. According to the obtained results of previous research [36] gas pressure of 3 bars were fixed in the all experiments. The geometry

features of the top and boom kerf width were measured using Axioskop 40 optical microscope at a magnification of 50X and the images were exactly measured by the Imagej software. Figure 5. Shows the laser cutting process of polycarbonate samples. Figure 6 shows the influences of the input parameters variations on the kerf geometry of some selected experiments listed in table 2. Upper and lower picture of Figure 6 are top (T) and bottom (B) surface of the kerf width, respectively. T stands for top and B stands for bottom in the Figure 6.

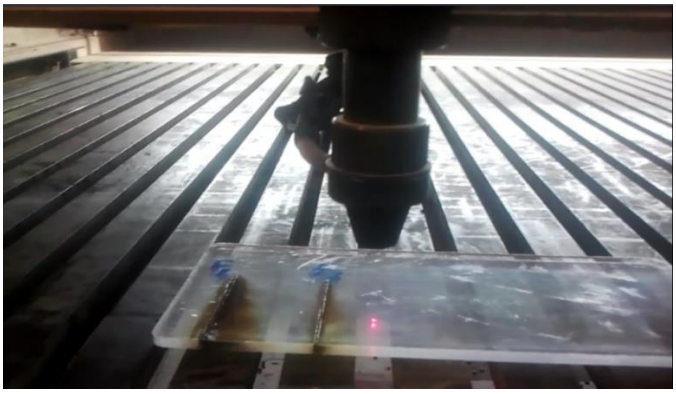

Figure. 5. The laser cutting process of polycarbonate samples

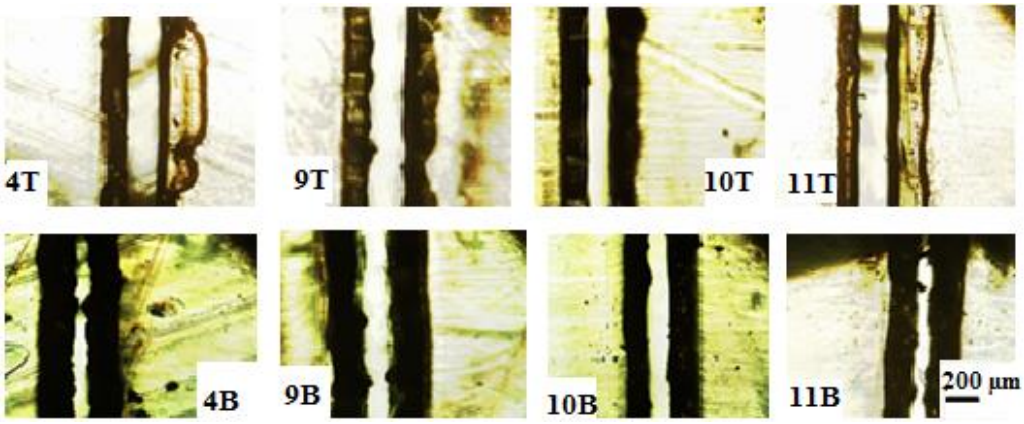

Figure. 6. Effect of the input parameters variations on kerf width geometry

There are several methods to measure the surface roughness which can be broadly divided into contact and non-contact types. In contact method the tip of the stylus directly touches the surface

of the sample. As the stylus traces across the sample, it rises and falls together with the roughness on the sample surface, Figure 7. This movement in the stylus is picked up and used to measure surface roughness. To measure the surface roughness (Ra) with profile meter, Equation 7 is used in which, the total area of the surface profile (Y(x) dx) is divided by the specified length L [37]. Contact method is used in the present research to measure the surface roughness of the kerf wall. Mahr-PS1 unit, a portable stylus type profile meter made-up by Maher Company, Germany, was used for surface roughness assessments. To achieve validity and accuracy, each Ra measurement was repeated three times along three different directions. The average of the three replications was then assigned as the surface roughness value for each treatment combination [38]. In all cases, a cutoff length of 0.8 mm and an evaluation length of 4 mm (5×0.8 mm) were adjusted on the unit according to ISO 4287/1.

$$R_a = \int_0^L |Y(X)|\, dx \qquad (7)$$

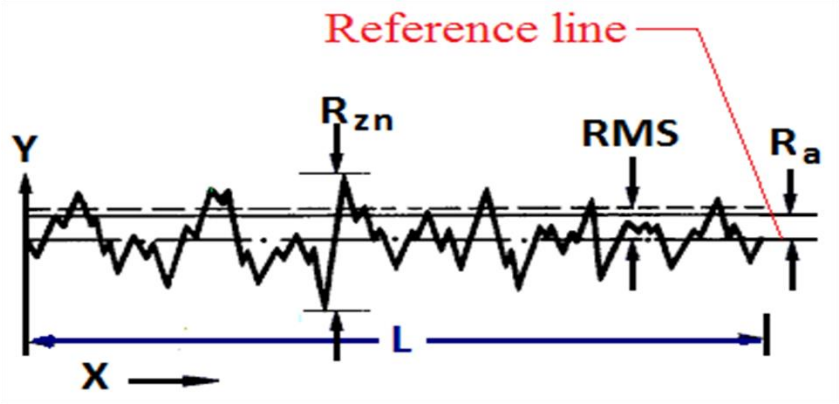

Figure. 7. Surface roughness profile of the kerf wall [37]

4. Results and discussion

The results of measuring the top and bottom kerf width, ratio of the upper kerf to lower kerf, heat affected zone (HAZ) and surface roughness were considered as the responses of the

experiment. Analysis of variance (ANOVA) was employed in order to investigate significant effective parameters on laser cutting process and interpretation of the results. In these analyses, full quadratic polynomial function was used.

4.1 Top kerf width

According to Analysis of variance on top kerf width, Table 3, the only linear effective parameter, is laser focal plane position (FPP). Among quadratic terms, the quadratic term of laser power (p^2) has a significant effect. Moreover, all the parameter interactions have significant effects on each other. The regression equation obtained is evaluated as significant and Lack-of-Fit as insignificant. In the best analysis, regression is to be significant and Lack-of-Fit insignificant. Therefore according to the analysis, the final regression in terms of coded parameter values yields in equation (8).

$$\text{Top kerf width } (\mu m) = 322.33 - 2.35\,S - 6.45\,P + 16.22\,FPP + 22.30\,P^2 - 41.48\,S\times P - 66.13\,S\times FPP + 43.10\,P\times FPP \quad (8)$$

Table 3 Revised analysis of variance of top kerf width

Source of variation	Degree of freedom	Sum of squares	Mean squares	F value	T value	P value
Model	7	5178.1	7368.3	18.25	-------	0.001
Linear	3	4469.8	1489.9	3.69	-------	0.070
S	1	71.3	71.3	3.69	-0.42	0.687
P	1	225.5	225.5	0.56	-0.75	0.479
FPP	1	3403.4	3403.4	8.43	2.90	0.023
Square	1	4524.7	4524.7	11.21	-------	0.012
P*P	1	4524.7	4524.7	11.21	3.35	0.012
2-Way Interaction	3	28016.0	9338.7	22.13	-------	0.001
S*P	1	9331.5	9331.5	23.11	-4.81	0.002
S*FPP	1	23718.7	23718.7	58.74	-7.66	0.000
P*FPP	1	10074.6	10074.6	24.95	5.00	0.002
Error	7	2826.5	403.8			
Lack-of-Fit	5	2731.6	546.3	11.52	-------	0.084
Pure Error	2	94.9	47.4			
Total	14	54404.6				
R-Sq = %94.80			R-Sq (adj) = % 89.61			

Figure 8 shows the top kerf width response surface on the basis of the input variables. As shown in Figure 8-a by decreasing the FPP value (locating the laser spot point in the depth of the specimen) the upper kerf reduces. When a focused laser beam is used in zero level of the FPP, (+2 in coded value equal zero in actual value), given that laser power would spread on the surface onto a wider area, hence more heat energy interact with the specimen and consequently the upper kerf increases [16].

Figure 8-b illustrates the variations of the top kerf width in terms of laser power and cutting speed. It is evident that the maximum top kerf width occurs in the maximum laser power and minimum cutting speed. It could be explained by the heat input value mentioned in Equation (9):

Heat in put = Laser power / Cutting speed (9)

Therefore by increasing the laser power and decreasing the cutting speed, heat input increases and more area of the material will be heated and melted, therefore the kerf width will become wider.

In samples number 8 and 9 cutting did not perform completely so none of the responses could not be measured, see Table 2. By using the concept of heat input, Equation 9, it could be explained. In these samples because of the lower laser power and higher cutting speed and locating the focal plane position on the or near the top surface, the energy of the laser beam is not sufficient for cutting performance. By comparing sample No 7 and 8 it could be realized that in both setting the cutting speed and laser power are the same, but the only difference is in focal plane positioning. In sample number 8 FPP is located in -3 mm below the top surface while in sample number 7 FPP is located -1 mm below the top surface. The same explanation given for

describing Figure 8-a could be discussed here also for creating kerf in sample 7 and no kerf in sample number 8.

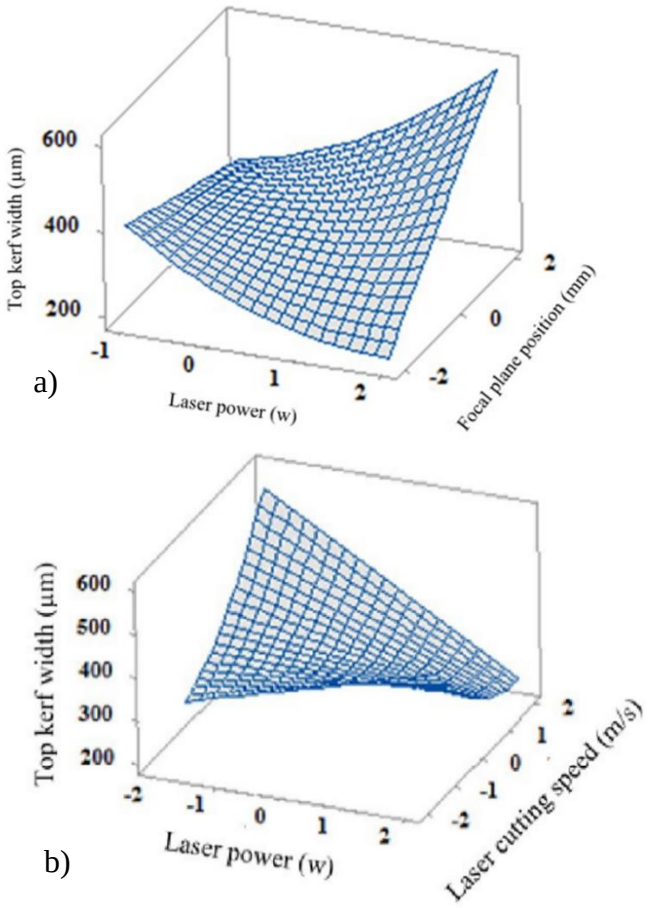

Figure. 8. Response surfaces of top kerf width in terms of a) laser power and focal plane position, b) laser power and laser cutting speed.

The Residual plot for top kerf width is displayed in Figure 9. As it is shown in the normal probability diagram, the response top kerf width, in comparison to others around the diagonal line, is scattered and shows a normal distribution. Therefore, the final extracted regression model is a suitable model for prediction and investigation of the effects of parameters in proportion to other responses. Thus, the result of mathematical equation is a desirable model to predict and investigate the effect of F and T using the experiment parameter.

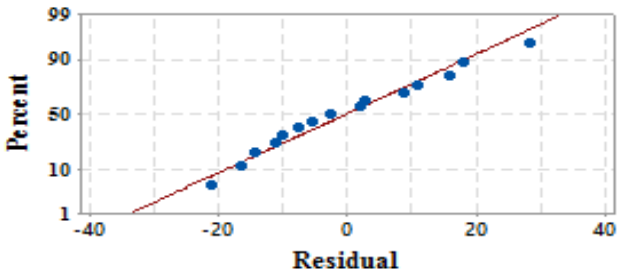

Figure. 9. The residual plot for top kerf width

4.2 Bottom kerf width

Table 4 shows analysis of variance for the bottom kerf width. As shown in Table 4, the main effective parameters are laser cutting speed (S) and laser focal plane position (FPP). Among quadratic terms, the quadratic term of laser power (P^2) and laser cutting speed (S^2) has a significant effect and interaction effect of cutting speed and laser focal plane position (S×FPP), laser power and focal plane position (P×FPP) were identified as the significant term. As Table 4 indicates, Lack-of-Fit was determined as insignificant and it shows that a suitable analysis has been performed. According to performed analyses in ANOVA table 4, equation 10 represents the regression equation for the bottom kerf width considering significant parameters based on coded values.

Bottom kerf width (μm) = 168.49 - 50.82 S - 12.38 P + 20.26 FPP + 27.03 S^2 + 28.08 P^2 - 42.57 S×FPP + 26.43 P×FPP (10)

Table 4 Revised analysis of variance of bottom kerf width

Source of variation	Degree of freedom	Sum of squares	Mean squares	F value	T value	P value
Model	7	89508.7	1287.0	32.72	-------	0.000
Linear	3	44692.1	14897.4	28.12	-------	0.000
S	1	35584.1	35584.1	91.07	-9.54	0.000
P	1	951.4	951.4	2.43	-1.56	0.163
FPP	1	5756.5	5657.5	14.48	3.81	0.007
Square	2	21069.4	10534.7	26.96	-------	0.001
S*S	1	17753.6	17753.6	42.88	6.55	0.000
P*P	1	7458.4	7458.4	19.09	4.37	0.003
2-Way Interaction	2	12626.0	6313.0	16.16	-------	0.002
S*FPP	1	10966.8	10966.8	28.07	-5.30	0.001
P*FPP	1	4227.9	4227.9	10.82	3.29	0.013
Error	7	2753.3	390.4			
Lack-of-Fit	5	4227.1	485.4	3.15	-------	0.258
Pure Error	2	308.2	154.1			
Total	14	92244.0				
R-Sq = % 97.03			R-Sq (adj) = % 94.07			

Figure 10 illustrates the bottom kerf width response surface on the basis of the input variables. In Figure 10-a it should be noted that the linear influence of the cutting speed even changes sign. The effect of the cutting speed on bottom kerf width in the minimum level of FPP is more than its influence in the maxmimum level of FPP and of course with reverse effect. This is because of the intraction effect of these tow parameters.

It is clear in Figure 10-b that the lower the laser power and the higher the cutting speed will lead to reduction in bottom kerf width. Equation 9 could be helpful to clarify the reason. By reducing the heat input lower area of the material will be heated and melted, therefore the kerf width will become narrower.

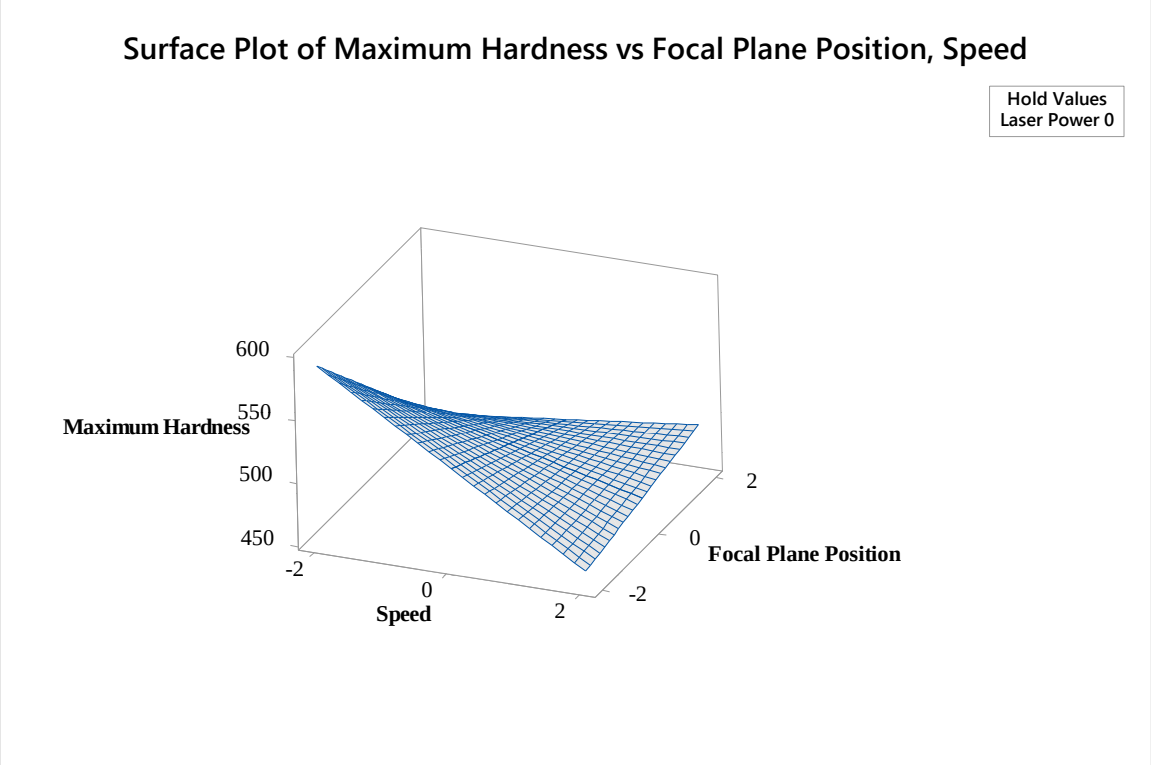

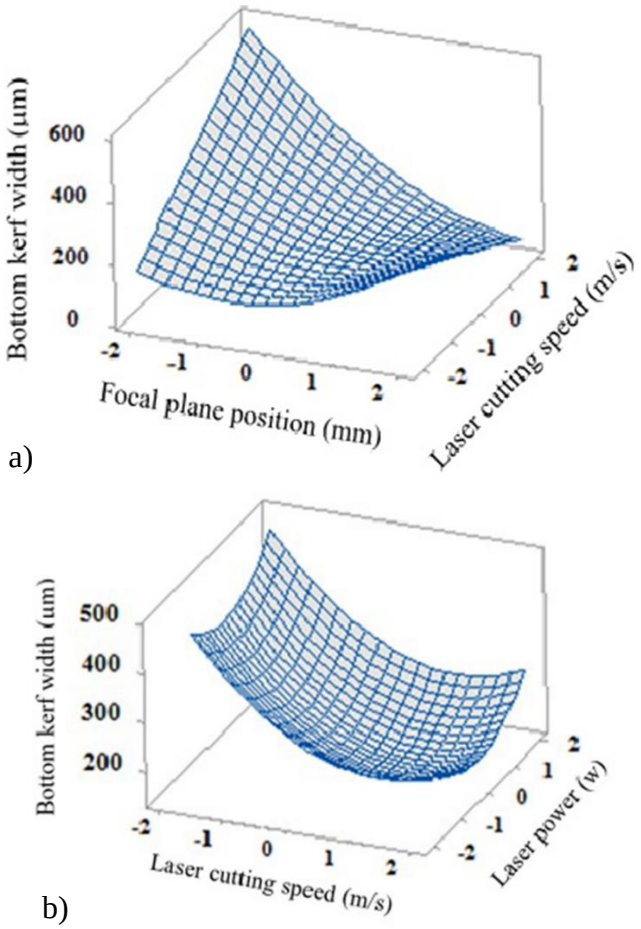

Figure. 10. Response surfaces of bottom kerf width in terms of a) Focal plane position and laser cutting speed, b) laser cutting speed and laser power

4.3 Ratio of the upper kerf to lower kerf

Table 5 shows variance analysis of the ratio of the upper kerf to lower kerf. The effective linear parameters are the laser cutting speed (S) and the focal plane position (FPP). The quadratic term of laser cutting speed (S^2) and laser power (P^2) have a significant effect and the only significant interaction effect is the laser cutting speed and the laser power (S×P). Final regression equation of the ratio of the upper kerf to lower kerf, based on the significant parameters, is shown in equation 10 based on coded values.

$$\text{Ratio} = 1.7044 + 0.2948\ S - 0.0198\ P - 0.1108\ FPP - 0.1041\ S^2 + 0.1071\ FPP^2 - 0.2031\ S\times P \quad (10)$$

Table 5 Revised analysis of variance of ratio top kerf to bottom kerf

Source of variation	Degree of freedom	Sum of squares	Mean squares	F value	T value	P value

Model	6	2.21076	0.36846	10.38	-------	0.002
Linear	3	1.36590	0.45540	12.83	-------	0.002
S	1	1.25396	1.25396	35.32	5.49	0.000
P	1	0.00368	0.00368	0.10	-0.32	0.756
FPP	1	0.17727	0.17727	4.99	-2.23	0.056
Square	2	0.17727	0.17727	10.05	-------	0.007
S*S	1	0.22622	0.22622	6.29	-2.51	0.036
FPP*FPP	1	0.23622	0.23622	6.65	2.58	0.033
2-Way Interaction	1	0.27101	0.27101	7.63	-2.76	0.025
S*P	1	0.27101	0.27101	7.63	-2.76	0.025
Error	8	0.28399	0.03550			
Lack-of-Fit	6	0.26594	0.04432	4.91	-------	0.179
Pure Error	2	0.01805	0.00902			
Total	14	2.49457				
R-Sq = % 88.62			R-Sq (adj) = % 80.08			

Ratio of the upper kerf to lower kerf response surfaces are displayed in Figure 11. In Figure 11-a it is evident that the FPP has a little effect on this response while the cutting speed has a large effect on it. According to both Figure 11 a and b it could be understand that minimum ratio occurs in the minimum cutting speed. It could be mentioned that due to the intraction effect of the cutting speed and the laser power the linear influence of the laser power changes sign in Figure 11-b.

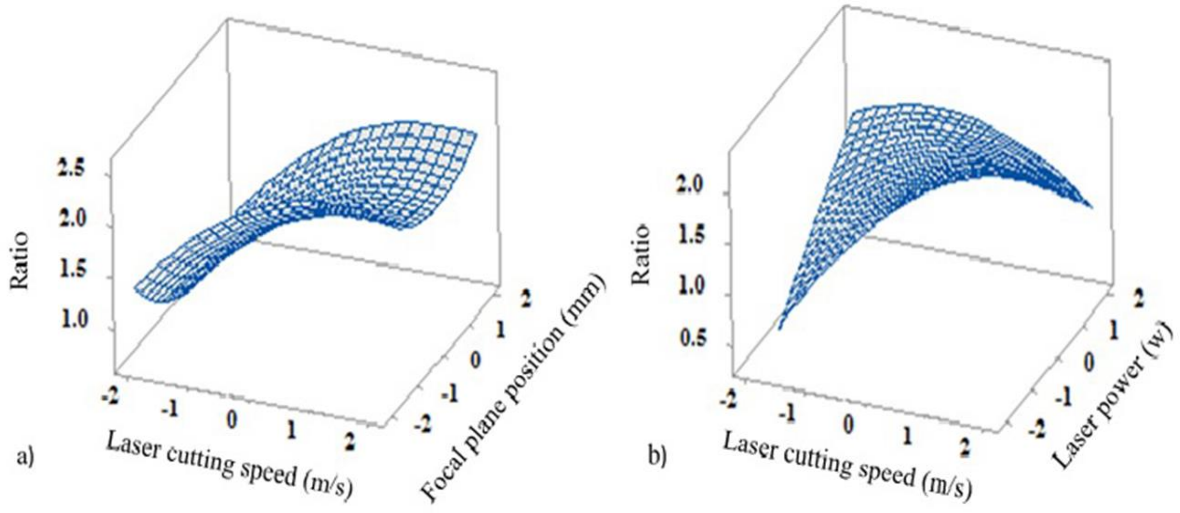

Figure. 11. Response surfaces of the ratio of the upper kerf to lower kerf in terms of a) laser cutting speed and focal plane position, b) laser cutting speed and laser power

4.4 Upper heat affected zone

According to the results of an analysis of variance runs on the upper heat affected zone, see Table 6, all parameters are significant except the FPP. Quadratic effect of the cutting speed (S^2) and the laser power (P^2) and interaction effect of the cutting speed and the laser power (S×P) are identified as significant terms. From the statistical analysis the Minitab software elaborated the following regression formula for the upper heat affected zone as a function of the varied process parameters:

Upper heat affected zone (µm) = 268.40 - 44.66 S + 21.33 P + 9.97 FPP + 14.88 S^2 - 21.70 P^2 + 27.91 S×P (11)

Table 6 Revised analysis of variance of heat effected zone

Source of variation	Degree of freedom	Sum of squares	Mean squares	F value	T value	P value
Model	7	39762.4	5496.6	19.21	-------	0.000
Linear	3	27977.0	9325.7	31.21	-------	0.000
S	1	27481.0	27481.1	92.69	-9.63	0.000
P	1	2825.1	2825.8	9.53	3.09	0.018
Square	2	11436.1	5718.0	19.29	-------	0.001
S*S	1	5075.0	5075.0	17.12	4.14	0.004
P*P	1	4456.6	4456.6	15.03	-3.88	0.006
2-Way Interaction	2	5201.2	2600.6	8.77	-------	0.012
S*P	1	4712.8	4712.8	15.90	3.99	0.005
Error	7	2075.4	296.5			
Lack-of-Fit	5	1522.9	304.6	1.10	-------	0.539
Pure Error	2	552.5	276.4			
Total	14	41937.9				
R-Sq = % 86.3			R-Sq (adj) = % 82.2			

Response surfaces and contour plots of upper heat affected zone are illustrated in Figure 12 and 13, via the input parameters. As mentioned in explanation of ANOVA table 6, Figure 12 confirms that the FPP has an ignorable effect while the cutting speed has a highly revers influence on upper heat affected zone [17]. By using the concept mentioned in Equation 9 the behavior of the cutting speed and the laser power in Figure 13 could be explained. The minimum upper heat affected zone occurs when the laser power is at the minimum level and the cutting speed is at the highest level. In this condition the heat input reduces, see Equation 9. Therefore less laser energy interact to the material. Thus the upper heat affected zone reduces [20]. The vice versa condition, high laser power and low cutting speed, result in increasing the upper heat affected zone.

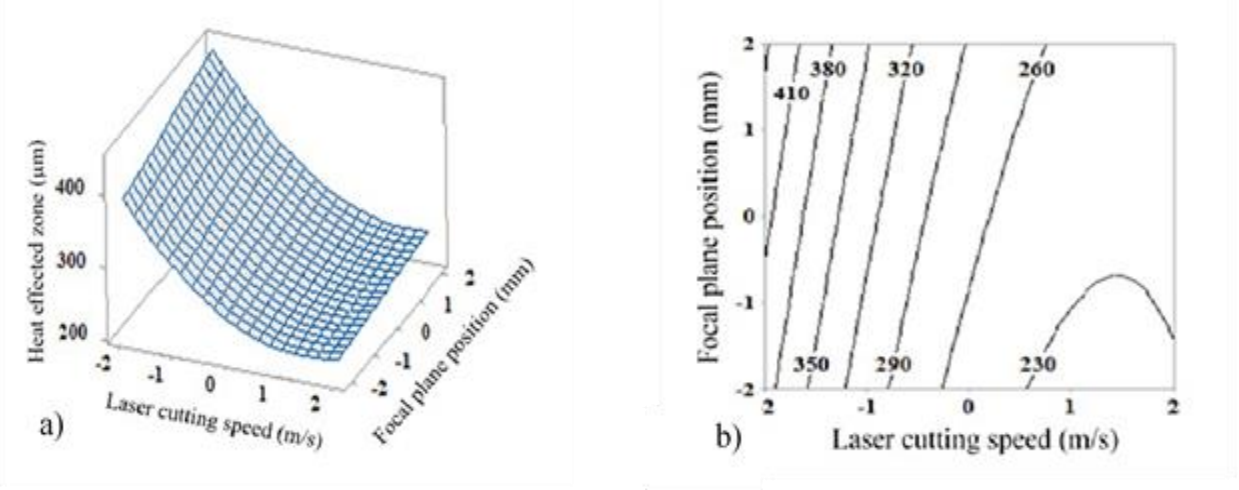

Figure. 12. a) Response surface and b) contour plot of upper heat effected zone in terms of laser cutting speed and focal plane position

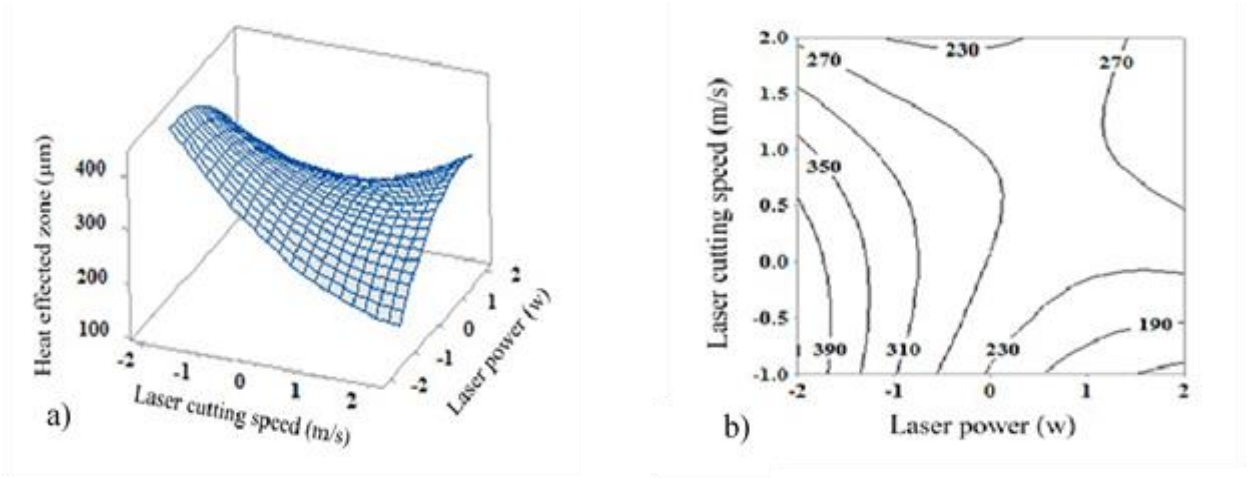

Figure. 13. a) Response surface and b) contour plot of upper heat effected zone in terms of laser cutting speed and laser power

4.5 Surface roughness of the kerf wall

According to Analysis of variance on surface roughness of the kerf wall, table 7, the effective parameters, are the laser power (P) and the focal plane position (FPP). Among quadratic terms, the quadratic term of the cutting speed (S^2) has a significant effect and interaction effect of the cutting speed and the laser power (S×P), cutting speed and focal plane position (S×FPP), laser power and focal plane position (P×FPP) were identified as the significant terms. Therefore according to the analysis, the final regression in terms of coded parameter values yields in equation (12).

$$Ra\ (\mu m) = 4.957 + 0.178\ S - 0.632\ P + 0.519\ FPP + 0.371\ S^2 - 1.969\ S\times P - 1.816\ S\times FPP + 1.066\ P\times FPP \quad (12)$$

Table 7 Revised analysis of variance of surface roughness of the kerf wall

Source of variation	Degree of freedom	Sum of squares	Mean squares	F value	T value	P value
Model	3	51.1732	7.3105	13.22	-------	0.001
Linear	3	9.2061	3.0687	5.55	-------	0.029
S	1	0.4262	0.4262	0.77	0.88	0.409
P	1	3.4695	3.4695	6.27	-2.50	0.041
FPP	1	3.6265	3.6265	6.56	2.56	0.038
Square	1	3.24.49	3.24.49	5.86	-------	0.046
S*S	1	3.24.49	3.24.49	5.86	2.42	0.046
2-Way Interaction	3	33.02.26	11.0075	19.90	-------	0.001
S*P	1	22.4533	22.4533	40.59	-.6.37	0.000
S*FPP	1	19.1094	19.1094	54	-5.88	0.001
P*FPP	1	6.5853	6.5853	11.90	3.45	0.011

Error	7	3.8723	0.5532			
Lack-of-Fit	5	2.3739	0.4748	0.63	-------	0.706
Pure Error	2	1.4985	0.7492			
Total	14	55.0455				
R-Sq = %92.97			R-Sq (adj) = % 85.93			

Surface roughness of the kerf wall response surfaces are displayed in Figure 14. Because of the interaction of the cutting speed and the focal plane position demonstrated in the Figure 14(a), the best surface roughness of the kerf wall attains in the lowest cutting speed and focal plane position levels. When the cutting speed is low and focal plane positioned in the middle of the workpiece thickness, the melted materials removes uniformly. Thus, on the surface of the kerf wall the distance between peak and troughs decreases, see Figure 6. It could be said that because of the intraction effect of the parameters the linear influence of the cutting speed changes sign in Figure 14 (a) and 14(b).

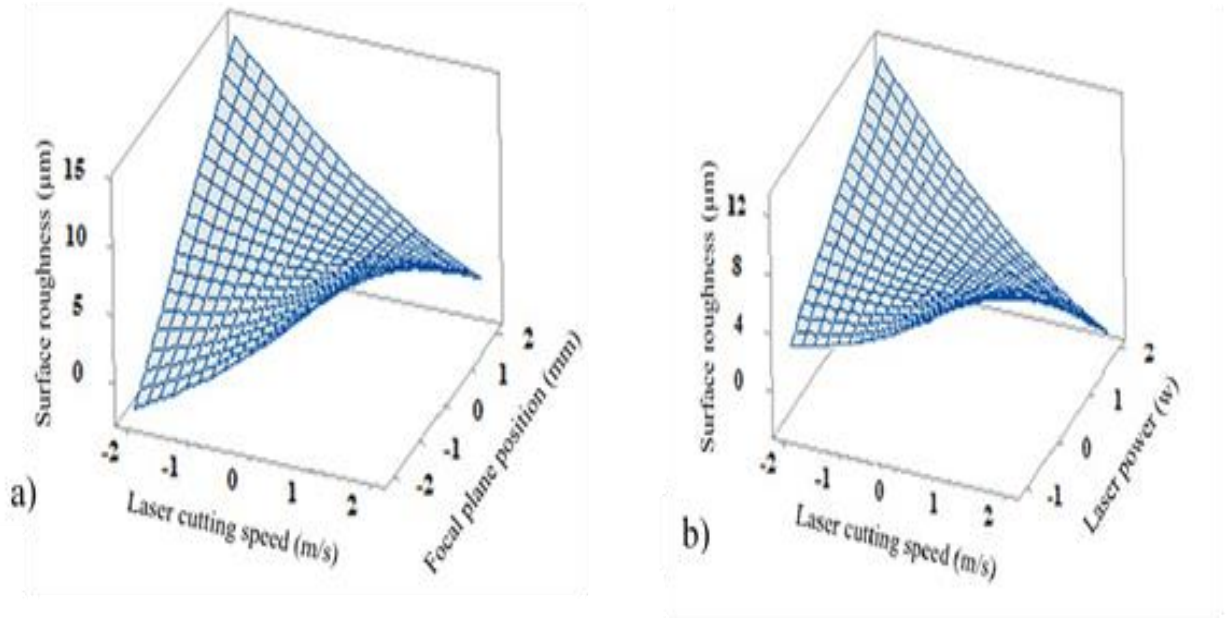

Figure. 14. Response surfaces of surface roughness of the kerf wall in terms of a) laser cutting speed and focal plane position, b) laser cutting speed and laser power

5. Optimization

By statistical analysis of obtained data from experimental tests, regression's equations explain logical relations between input variables and responses. The response optimizer option within the DOE module of Minitab statistical software package, release 17, has been used here to optimize input parametric combinations resulting in the most desirable compromise between different responses using desirability function as mentioned in section 2.2. Table 8 summarizes criterions in order to optimize process parameters. Minimum top kerf width, Minimum heat effect zone, minimum surface roughness and ratio of top kerf width to bottom kerf width equal to 1 are the criteria of the optimization.

Table 8 Constraints and criteria of input parameters and responses

	Parameter/Response		Goal	Lower	Target	Upper	Weight	Importance
Parameters		Speed	Is in range	2	---	18	---	---
		Power	Is in range	20	---	40	---	---
		FPP	Is in range	-4	---	-1	---	---
Response	Criteria 1	Ratio	Target 1	0.7894	1	2.5161	1	5
	Criteria 2	Ratio	Target 1	0.7894	1	2.5161	1	5
		Roughness	Minimize	2.15	---	9.74	1	5
	Criteria 3	Kerf top	Minimize	265.3061	---	518.3673	1	5
		Ratio	Target 1	0.7894	1	2.5161	1	5
		Roughness	Minimize	2.15	---	9.74	1	5
	Criteria 4	Kerf top	Minimize	265.3061	---	518.3673	1	5
		HAZ Top	Minimize	178.67	---	420.4082	1	5
		Ratio	Target 1	0.7894	1	2.5161	1	5

	Criteria 5	Kerf top	Minimize	265.3061	---	518.3673	1	5
		HAZ Top	Minimize	178.67	---	420.4082	1	5
		Ratio	Target 1	0.7894	1	2.5161	1	5
		Roughness	Minimize	2.15	---	9.74	1	5

In the optimization procedure presented in table 8, the weight and importance values of the responses are mentioned. Verification experiments were performed at the obtained optimal input parametric setting to compare the actual top kerf width, heat effect zone, ratio and surface roughness with those as optimal responses obtained from optimization. Table 9 presents the optimization results along with experimentally obtained responses and their percentage relative verification errors. It is clear that the error percentage of the study is good for engineering applications. Because of minimum error and better quality of the kerf the criteria number 4 and 5 which have the same optimization setting as mentioned in Table 9 are selected for the best condition of this process.

Table 9 Optimum prediction results and experimental validation

Solution		Optimum input parameters			Composite Desirability		Output responses			
		S	**P**	**FPP**			**Ra**	**Ratio**	**Ker Top**	**HAZ Top**
1	Coded Value	2	2	0.3434	0.9085	Actual		1.130		
						Predicted	---	1.0002	----	---
	Actual Value	18	40	-1.6566		Error %		%13		
2	Coded Value	-1.9727	-0.9653	-2	1	Actual	3.62	1.15		
						Predicted	3.2354	1	---	---
	Actual Value	2.1092	25.1735	-4		Error %	%12.3	%15	---	----

3	Coded Value	-1.9727	-0.9653	-2	1	Actual	3.55	1.120	72.9458	---
	Actual Value	2.1092	25.1735	-4		Predicted	3.2354	1	64.8177	---
						Error %	%10	%12	%12.54	
4	Coded Value	1.5556	2	0.2222	0.7928	Actual	---	1.373	296.790	311.555
	Actual Value	16.2224	40	-1.7778		Predicted	---	1.2203	265.8411	279.1719
						Error %	---	%12.55	%11.6	%11.6
5	Coded Value	1.5556	2	0.2222	0.8523	Actual	1.60	1.35	299.555	306.647
	Actual Value	16.2224	40	-1.7778		Predicted	1.2953	1.2203	265.8411	279.1719
						Error %	%23.52	%10.78	%12.68	%9.84

Conclusions:

In the present paper, the process of laser cutting was performed using low power CO2 laser on injected polycarbonate sheet with thickness of 3.2mm. Laser cutting speed, laser power and focal plane position are considered as the process input parameters and kerf geometry dimensions and surface roughness of the kerf wall are considered as the process output responses. The obtained data from the experiments were analyzed through design of experiments (DOE). Results Showed that increasing laser power and position of the focal plane, increases the upper kerf width while revers condition occurs for speed of laser cutting on this response. Also increasing the cutting speed increases the kerf ratio. Obtained results also demonstrated that increasing in the cutting speed and reduction in the laser power lead to decrease the upper heat affected zone. Besides in the higher laser power and the lower cutting speed, surface roughness decreases. However as a general result, by locating the laser spot point in the depth of the workpiece the laser cutting quality increases. Furthermore by performing an optimization process, using desire ability approach, the following settings can be described as the optimum settings of the laser cutting

process of polycarbonate sheet with the thickness of 3.2 mm: cutting speed (S) = 16 mm/s, laser power (P) = 40 W, focal plane position (FPP)= -1.8 mm.

References:

[1] Tamrin K.F, Nukman Y, Choudhury I.Y, Shirley S. Multiple-objective optimization in precision laser cutting of different thermoplastics. Optics and Lasers in Engineering 2015; 67: 57–65.

[2] Elijah Kannatey, Asibu JR. Principles of laser material processing.3th Ed. New Jersey; Published by John: 2009.

[3] Eltawahni HA, Benyounis KY, Olabi AG. High Power CO_2 Laser Cutting for Advanced Materials–Review.1th ed. Irland; Elsevier, chapter book: 2016.

[4] Happer, Charles A. handbook of plastics elastomers and composites plastics engineering. Department New York; university of Massachusetts Lowell: 2004.

[5] AM Oladoye, JG Carton, K Benyounis, J Stokes, AG Olabi. Optimisation of pack chromised stainless steel for proton exchange membrane fuel cells bipolar plates using response surface methodology Surface and Coatings Technology 2016; 304: 384-392.

[6] Moradi M, Golchin E. Investigation on the effects of process parameters on laser percussion drilling using finite element methodology; statistical modelling and optimization. Latin American Journal of Solids and Structures 2017; 14: 464 – 484.

[7] Mahmoud Moradi, Hadi Abdollahi. Laser Percussion Micro-Drilling on Thin Stainless Steel Sheet AMS 5510; Statistical Modelling and Optimization. Journal of lasers in Engineering 2017; 39:385-495.

[8] Moradi M, AbbasiRad M, Ghoreishi M, Abdollahi M, Rostami M. Investigation and Optimization of EDM Milling and its Comparison with Die Sink EDM. International Journal of Advanced Design and Manufacturing Technology (ADMT) 2017. Article in press.

[9] Khorram A, Soleymani Yazdi M.R, Ghoreishi M, Moradi M. Using ANN Approach to Investigate the Weld Geometry of Ti 6Al 4V Titanium Alloy. International Journal of Engineering and Technology 2010; 2: 488-495.

[10] Olabi AG, Casalino G, Benyounis KY, Hashmi MSJ. An ANN and Taguchi algorithms integrated approach to the optimization of CO 2 laser welding. Advances in Engineering Software 2006; 37: 643-648

[11] Singh Yadav B, Pokhariyal Barkha Ratta M, Rai G, Saxena M, Sharma M, Mishra K.P. Predicting secondary structure of Oxidoreductase protein family using Bayesian Regularization Feed-forward Backpropagation ANN Technique. Journal of Proteomics and Bioinformatics 2010; 35: 179-182.

[12] Zhou BH, Mahdavian SM. Experimental and theoretical analyses of cutting nonmetallic materials by low power CO_2 laser, Journal of Materials Processing Technology 2004; 146: 188–192.

[13] Pathik P, Piyush G, Shilpesh R. Laser Machining of Polymer Matrix Composites Scope, Limitation and Application. International Journal of Engineering Trends and Technology 2013; 4: 2391-2399.

[14] Pathik P, Saurin S, Tejas P. Experimental Analysis and ANN Modelling of HAZ in Laser Cutting of Glass Fibre Reinforced Plastic Composites, 3rd International Conference on Innovations in Automation and Mechatronics Engineering 2016; 23: 406-413.

[15] Ohkuboa T, Tsukamotob M, Satob Y, Numerical Simulation of Laser Beam Cutting of Carbon Fiber Reinforced Plastics, Physics Procedia 2014; 56: 1165-1170.

[16] Eltawahni HA, Benyounis KY, Olabi AG. Effect of process parameters and optimization of CO2 laser cutting of ultrahigh-performance polyethylene, Materials and Design 2010; 31: 4029–4038.
[17] Pathik P, Saurin S, Bhavin M, Tejas P. Experimental Analysis and Prediction of Kerf width in Laser Cutting of Glass Fibre Reinforced Plastic Composite Material. Proceedings of International Conference on Advances in Materials Manufacturing and Application 2015; 24: 139-146.
[18] Karimzad Ghavidel A, Azdast T a, Shabgard MR, Navidfar A, Mamaghani Shishavan S. Effect of carbon nanotubes on laser cutting of multi-walled carbon nanotubes/poly methyl methacrylate Nano composites. Optics and Laser Technology 2015; 67: 119–124
[19] Choudhury IA, Chuan PC. Experimental evaluation of laser cut quality of glass fiber reinforced plastic composite. Optics and Lasers in Engineering 2013; 51: 1125–1132.
[20] Eltawahni HA, Benyounis KY, Olabi AG. Investigating the CO2 laser cutting parameters of MDF wood composite material. Optics and Laser Technology 2011; 43: 648–659.
[21] Eltawahni HA, Rossini NS, Dassisti M, Alrashed K, Aldaham TA, Benyounis KY, Olabi AG. Evalaution and optimization of laser cutting parameters for plywood materials. Optics and Lasers in Engineering 2013; 51:1029-1043.
[22] Eltawahni HA, Benyounis KY, Olabi AG. Assessment and optimization of CO2 laser cutting process of PMMA. International conference on advances in materials and processing technologies 2010; 1315: 1553-1558.
[23] Eltawahni HA, Hagino M, Benyounis KY, Inoue T, Olabi AG. Effect of CO_2 laser cutting process parameters on edge quality and operating cost of AISI316L. Optics and Laser Technology 2012; 44:1068-1082.
[24] Herzog D, Schmidt-Lehr M, Oberlander M, Canisius M, Radek M, Emmelmann C. Laser cutting of carbon fibre reinforced plastics of high thickness. Materials and Design 2016; 92: 742–749.
[25] Dalibor Petkovic, Vlastimir Nikolic, & Miloš Milovancˇevic, & Lyubomir Lazov. (2016). "Estimation of the most influential factors on the laser cutting process heat affected zone (HAZ) by adaptive neuro-fuzzy technique," *Infrared Physics & Technology*, vol. 77, pp. 12-15
[26] Riveiro A, Quintero F, Lusquiños F, del Val J, Comesaña R, Boutinguiza M, Pou J. Experimental study on the CO2 laser cutting of carbon fiber reinforced plastic composite. Composites Part 2012; 43: 1400–1409.
[27] Moradi M, Ghoreishi M, Influences of Laser Welding Parameters on the Geometric Profile of Ni-Base Superalloy Rene 80 Weld-Bead. International Journal of advanced manufacturing Technology 2011; 55: 205-215.
[28] Azadi M, Azadi S, Zahedi F, Moradi M. Multidisciplinary optimization of a car component under NVH and weight constraints using RSM. International Mechanical Engineering Congress and Exposition 2009; 15:315-319.
[29] Khuri, Andre I., Cornell, John A. Response Surfaces: Designs and Analyses: Second Edition. Folorida: Taylor Francis: 1996.
[30] Moradi M, Ghoreishi M, Frostevarg J, Kaplan A. An investigation on stability of laser hybrid arc welding. Optics and Lasers in Engineering 2013; 51: 51 481-487.
[31] Moradi M, Salimi N, Ghoreishi M, Abdollahi H, Shamsborhan M, Frostevarg J, Ilar T, Kaplan A. Parameter dependencies in laser hybrid arc welding by design of experiments and by a mass balance. Journal of Laser Applications 2014; 26: 022004-1-9.
[32] Moradi M, Mohazabpak A. Statistical modelling and optimization of laser percussion micro-drilling on Inconel 718 sheet using response surface methodology. Journal of lasers in Engineering 2017, Volume 39, Issue 4-6.
[33] Derringer G, Suich R. Simultaneous Optimization of Several Response Variables. Journal of Quality Technology 1980; 12: 214-219.
[34] Moradi M, Ghoreishi M, Torkamany MJ. Modeling and optimization of nd:yag laser-tig hybrid welding of stainless steel. Journal of lasers in Engineering 2014; 27: 211–230.
[35] Watson M N, Oakley PJ, Dawes CJ. Laser welding techniques and testing. 2th Ed. New York; British Maritime Technology: 1985.

[36] Moradi M, Mehrabi M, Azdast T. Benyouniss KY. The effect of low power CO_2 laser cutting process parameters on polycarbonate cut quality produced by injection molding. Journal of Modares Mechanical Engineering 2017. 17 (2), 93-100.
[37] Dashtizadeh M, Biglari FR. Surface metrology and contact roughness measurement. 2th ed. Tehran; in persion Amirkabir University of Technology: 2005.
[38] Assarzadeh S, Ghoreishi M. Statistical Investigation into the Effects of Electro-Discharge Machining Parameters on WC/6%Co Composite-Part Modeling through Response Surface Methodology (RSM). Advanced Materials Manufacturing and Characterization 2013; 3: 210-116.